Online ISSN: 2981-0396 Print ISSN: 2981-0388

International Journal of Iron & Steel Society of Iran

Journal Homepage: https://journal.issiran.com/

Research Article

Investigating the effect of hardness, size, and position of inclusions on the fatigue strength of the steel AISI 304

V. Ghaffari Aliabad [1], A. R. Mashreghi *[2], A. Seyfoddini [3]

Department of Mining and Metallurgical Engineering, Yazd University, University Blvd, Safayieh, Yazd, Iran

ARTICLE INFO

Keywords:

Fatigue, AISI 304 steel, Non-metallic inclusions, Stress intensity factor, Fatigue limit.

Article history:

Received 30 December 2023
Received in revised form 19 February 2024
Accepted 09 March 2024

ABSTRACT

One of the most crucial factors influencing the strength and quality of steels is the presence of non-metallic inclusions. Studies demonstrated that non-metallic inclusions in industrial parts diminish their fatigue strength. On the other hand, their hardness is another influential parameter affecting the fatigue strength of steels. Therefore, this research investigated the impact of non-metallic inclusions on the fatigue strength of AISI 304 steel with three hardness of 170, 250, and 330 Vickers. This research revealed that as the hardness decreases, the fatigue strength of the part also decreases. Additionally, an examination of the failure surfaces of the parts using scanning electron microscopy (SEM) indicates that non-metallic inclusions are the root cause of fatigue failure in the samples. Finally, employing Murakami relations, parameters such as stress intensity factor and critical inclusion size were determined for steel with hardness levels of 170, 250, and 330 Vickers. The critical inclusion size for steel with hardness levels of 170, 250, and 330 Vickers was calculated as 32.7, 24.8, and 15 micrometers, respectively.

1. Introduction

Today, between 80 to 90% of part failures are due to fatigue [1]. Fatigue failure has various reasons, the most important of which are surface roughness, microstructure, size and position of inclusions, sample hardness, surface residual stresses, etc. [2, 5]. The existence of non-metallic inclusions is one of the biggest problems for steel producers. The formation of non-metallic inclusions occurs during the steel production process, and these inclusions significantly affect the mechanical properties of steel [6, 7]. Most non-metallic inclusions consist of oxide and sulfide compounds.

Given that, almost all fatigue failures start from points with stress concentration, and since non-metallic inclusions are also one of the sources of stress concentration in industrial parts, investigating these inclusions and their effect on the fatigue strength of steel is of great importance. On the other hand, hardness is an important parameter in determining steel's fatigue limit [8-13]. Experimental results show that the fatigue strength of steels is directly related to their hardness. According to Murakami's findings, when Hv < 400 and the material is without defects, Eq. (1) can be used to determine the resistance of the steel structure against fatigue [14].

$$\sigma_{wm} = 1.6\ H_v \qquad \text{Eq.(1)}$$

In Eq. (1), σ_w is the laboratory sample's fatigue limit under the rotational bending test (R=-1), and H_v is Vickers hardness. When the cause of fatigue failure is the presence of non-metallic inclusions in part, the fatigue limit can be predicted using Eq. (2) [15].

*Corresponding author
Email: amashreghi@yazd.ac.ir
Address: Department of Mining and Metallurgical Engineering, Yazd University, University Blvd, Safayieh, Yazd, Iran
1. M.S. Student, 2. Associate professor, 3. Associate professor

http://10.22034/IJISSI.2024.2019093.1276
Published by ISSI (Iron & Steel Society of Iran)

$$\sigma_{wd} = \frac{1.43\ (Hv+120)}{(\sqrt{area})^{1/6}} \quad \text{Eq.(2)}$$

In Eq. (2), the area is equal to the area of the inclusion image perpendicular to the axis of applied stress.

This study aims to find a simple and efficient way to determine the fatigue limit of parts considering the effect of non-metallic inclusion as the main parameter of fatigue failure and using the Vickers hardness parameter. Therefore, Murakami et al. introduced the inclusion effective area parameter (√area) to investigate the effect of inclusion on fatigue strength quantitatively. Also, according to their results, the stress intensity factor, i.e. ($K_{I_{max}}$) at the inclusion location is calculated according to Eqs. (3) and (4) for surface and internal inclusions, respectively [15]:

$$K_{I_{max}} = 0.65\ \sigma_a \sqrt{\pi\sqrt{area}} \quad \text{Eq.(3)}$$

$$K_{I_{max}} = 0.5\ \sigma_a \sqrt{\pi\sqrt{area}} \quad \text{Eq.(4)}$$

In Eqs. (3) and (4), σ_a is equal to the stress on the inclusion, which is determined using Eq. (5) [15]:

$$\sigma_a = \sigma\ (1-\frac{2d}{D}) \quad \text{Eq.(5)}$$

In Eq. (5), σ is the applied stress on the sample, d is the distance of the inclusion from the sample surface, and D is the diameter of the laboratory sample [15].

On the other hand, the research results of many researchers [16-20] showed that reducing the inclusion size decreases the probability of fatigue failure of the part. On the other hand, these researchers found that there is a critical size for inclusion. If the size of inclusion in steel is smaller than this critical size, non-metallic inclusions are no longer the source of fatigue cracks. There are different methods to determine the essential size of inclusion. In this research, three extrapolation methods were used: Murakami's equations and the method proposed by Saberifar.

In the extrapolation method [21, 22], the diagram of inclusion size or (√area) leads to sample fracture according to the distance of the inclusions from the surface of the sample drawn. Then, to obtain the critical inclusion size, a line passes through two points below which there are no other points, and finally, this line is continued until it intersects the axis of the inclusion area. This method reports the intersection of the drawn line with the inclusion area axis as the critical inclusion size.

Some researchers have proposed Eq. (6) using Murakami's equations to predict the critical inclusion size [21].

$$\phi = C\ (1 + \frac{120}{H_V})^6 \quad \text{Eq.(6)}$$

In this equation, ϕ is equal to the critical inclusion diameter in micrometers, and C is a constant number for three internal, surface, and subsurface inclusions equal to 0.969, 0.813, and 0.528, respectively [21].

To predict the critical size of fatigue failure inclusion, Saberifar [23] proposed a new method based on stress concentration created by the inclusion that leads to failure. The obtained results show that the stress concentration parameter resulting from the inclusion leads to fatigue failure correctly describes the fatigue life of the sample. Because stress intensity factor $K_{I_{max}}$ includes the inclusion size. Therefore, it is considered the best option for predicting the critical inclusion size of the fatigue part. As a result, the critical inclusion size can be obtained by replacing the essential value of the parameters in this relationship. In this regard, first, the smallest value of the stress intensity factor among the tested samples, i.e., $K`_{I_{max}}$, is considered as the maximum resistance of the microstructure against the stress concentration caused by inclusions. On the other hand, the sample's fatigue limit is also considered the maximum acceptable stress to be applied to the piece. Therefore, due to surface inclusions being more destructive than other inclusions, Eq. (3) can be rewritten to determine the critical inclusion size as follows:

$$K`_{I_{max}} = 0.65\ \sigma_w \sqrt{\pi\sqrt{area_c}} \quad \text{Eq.(7)}$$

In this research, the maximum critical inclusion size was determined for AISI 304 steel with three hardnesses: 170, 250, and 330 Vickers, and the accuracy of the obtained numbers was investigated.

AISI 304 steel is placed in the category of chrome-nickel austenitic stainless steel. This steel has acceptable corrosion resistance due to low carbon and relatively high chromium and nickel, and it is also suitable for structures that require welding. Also, excellent toughness, high strength, and elongation are among the other advantages of AISI 304 steel, making it perform well in bending, deep drawing, cold forming, and rolling processes. As a result, this steel is widely used in various fields [24]. On the other hand, as mentioned, in the industry, between 80 to 90% of parts failure occurs due to mechanical fatigue. In addition, one of the most important factors of fatigue failure in steel parts is the presence of non-metallic inclusions. On the other hand, hardness is another parameter influencing the fatigue strength of steels. As a result, in this research, the effect of hardness, size, and location of non-metallic inclusions on the fatigue strength of AISI 304 steel has been investigated.

2. Research materials and methods

In this study, samples of AISI 304 steel were made according to the DIN 50113 standard to perform the fatigue test. In Fig. 1. the map of the manufactured samples can be seen. The chemical composition of the raw material is given in Table 1. Also, to check the effect of hardness in this study, samples were subjected to annealing heat treatment until samples with three hardness of 170, 250, and 330 Vickers were prepared. Table 2. shows the heat treatment process. The fatigue test was also performed with a rotating-bending device at a speed of 5800 rpm and a stress ratio of R=-1. The test was continued until the sample broke or completed 2×10^6 cycles. The fracture surfaces of the samples were examined using a Scanning Electron Microscope (SEM) to investigate the inclusion location, size, and its effect on fatigue strength as a failure factor. All the broken samples were examined under the SEM microscope to determine the value of √area, and after determining the inclusion that caused the failure, its dimensions were measured. If the cross-section of the impurity in the fracture plane is close to a circle, the formula for calculating the area of a circle is used. If it is similar to an ellipse, the elliptic relation is used to calculate the square of the area.

3. Results and Discussion

3.1. S-N diagram

Fig. 2. shows the S-N diagram from the fatigue test for all the examined samples. Since the stress at which the sample can withstand 2×10^6 cycles without breaking is called the fatigue limit or σ_w, the samples that endured this number of cycles in this test were separated from the machine.

According to this diagram, the fatigue limit for steel with a hardness of 330 is equal to 385 MPa; for steel with a hardness of 250 Vickers, it is equal to 355 MPa; and for steel with a hardness of 170 Vickers, it is equal to 225 MPa. Therefore, according to the obtained results, samples with a hardness of 330 Vickers have higher strength than samples with a hardness of 250 Vickers, and samples with a hardness of 250 Vickers have a higher strength than samples with a hardness of 170 Vickers. In conclusion, these results clearly show that the fatigue strength of the samples is directly related to their Vickers

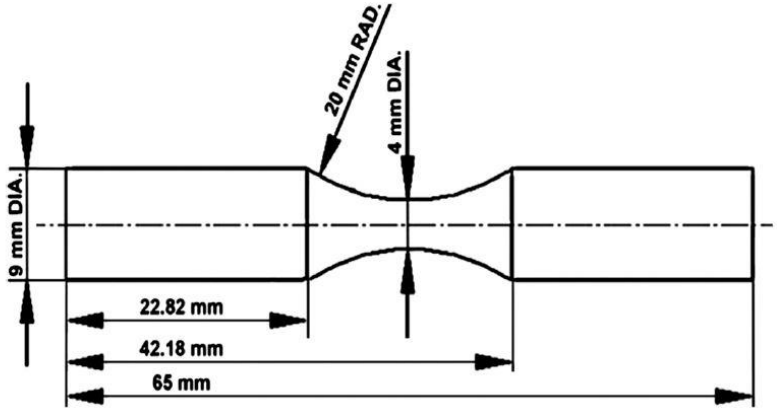

Fig. 1. Standard example of fatigue test.

Table 1. Chemical composition of used AISI 304 stainless steel.

Element	V	Ni	Mo	Cr	Si	Mn	C
wt%	0.051	8.815	0.191	18.388	0.46	0.909	0.068
Element	N_2	Nb	Al	Ti	Co	Cu	W
wt%	0.032	0	0.006	0.002	0.083	0.322	0.018

Table 2. Annealing process and hardness of tested steels.

Sample Hardness (HV)	Annealing time (minutes)	Annealing temperature (°C)
330	As received	
250	5	900
170	120	1100

hardness, and the higher the Vickers hardness of the material, the higher its fatigue strength will be.

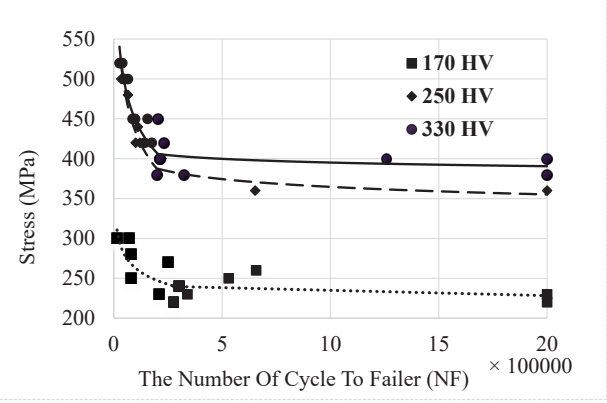

Fig. 2. The S-N diagrams obtained from the fatigue test of specimens.

3.2. Fractography

The failure surfaces of all the fatigue test samples were investigated using a scanning electron microscope (SEM). In general, the surface of each sample includes three areas, namely, crack initiation, crack propagation, and the final fracture area, which can be seen in Fig. 3. To investigate the cause of fatigue failure, the crack initiation was examined in high magnifications. The images of fatigue crack initiation well show that inclusion is the cause of crack creation and propagation in most samples. In Fig. 4. an example of including the fracture agent can be seen at the place of crack initiation.

It should be noted that in some examples, only one inclusion is not the cause of crack initiation. Still, several inclusions located near each other, called inclusion colonies, cause crack initiation. Inclusion colonies have a more destructive effect than a single inclusion and cause

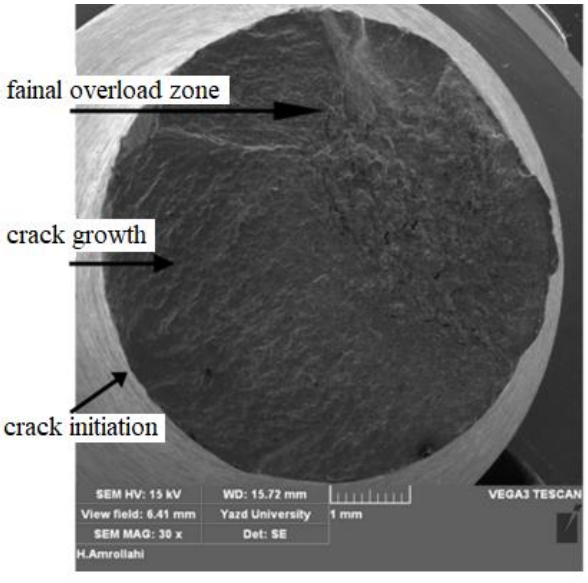

Fig. 3. Three zones of fatigue failure in a sample.

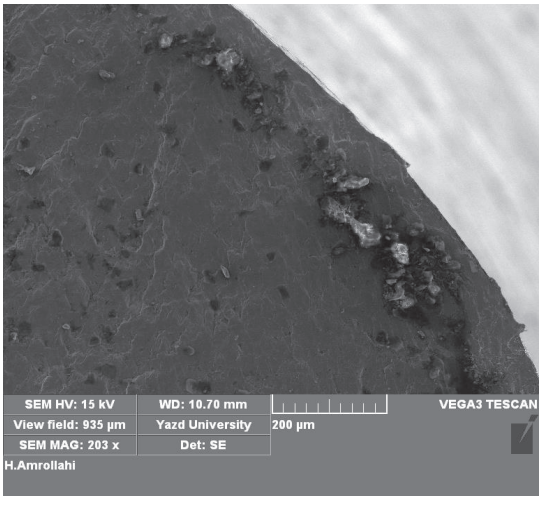

Fig. 4. Inclusion image of fatigue crack initiation agent.

premature component failure. Fig. 5. shows an example of the colony inclusions causing part fatigue failure.

3.3. Stress intensity factor at the crack initiation site

In Tables 3, 4, and 5. the information obtained from the observations of inclusions at the place of fatigue crack initiation site and the results of the calculations of Murakami's proposed parameters are given for samples with a hardness of 170, 250, and 330 Vickers, respectively. According to these tables, except in four cases, the ratio of the stress on the inclusion to the fatigue limit, σ_a/σ_w, is more significant than one in all the samples, and therefore, this issue justifies the failure of the fatigue samples due to the inclusion. But regarding those four exceptions, firstly, the numbers obtained for σ_a/σ_w are very close to one, and as a result, there is a possibility that the test error is the cause of this phenomenon. In addition, microcracks around the inclusions are also one factor that may cause the part's premature failure.

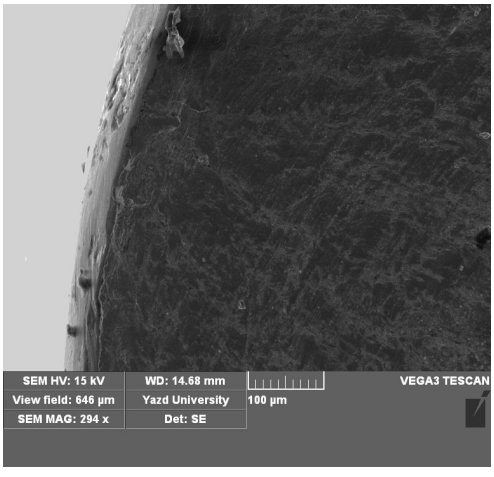

Fig. 5. An example of inclusion accumulation at the fatigue crack initiation site.

Table 3. Fatigue test results for AISI 304 steel samples with a hardness of 330 Vickers.

Stress (MPa)	Number of cycles	Place of departure	d (μm)	$\sqrt{area}$ (μm)	Stress on inclusion (MPa)	$K_{I_{max}}$ (MPa$\sqrt{m}$)	σ_a/σ_w
520	39157	Internal	45.48	60.64	508.17	3587.58	1.32
520	30503	Internal	10.15	57.08	517.36	3503.54	1.34
520	26134	Superficial	0	45.07	520	4020.77	1.35
500	64781	Superficial	0	31.84	500	3249.77	1.30
500	50094	Superficial	0	33.87	500	3351.82	1.30
500	47807	Superficial	0	39.23	1.30	3507.09	1.30
450	155587	Internal	3.37	17.15	449.24	1650.99	1.17
450	127871	Superficial	0	19.43	450	2285.10	1.17
450	86534	Internal	7.41	41.79	448.33	2577.40	1.16
420	233054	Internal	23.91	23.45	414.98	1802.04	1.08
420	175158	Internal	14.61	37.85	416.93	2289.34	1.08
420	142267	Internal [c]	119.15	76.04	409.53	3244.96	1.06
400	1258561	Internal	33.89	57.51	393.22	2687.48	1.02
400	211655	Superficial	0	66.15	400	3747.20	1.04
380	325682	Internal	104.40	119.61	360.16	3682.15	0.94
380	200396	Internal	105.46	18.14	351.96	4618.11	0.91

[C] In these tables, it stands for colony inclusion.

Table 4. Fatigue test results for AISI 304 steel samples with a hardness of 250 Vickers.

Stress (MPa)	Number of cycles	Place of departure	d (μm)	$\sqrt{area}$ (μm)	Stress on inclusion (MPa)	$K_{I_{max}}$ (MPa$\sqrt{m}$)	σ_a / σ_w
500	47106	Superficial	0	23.61	500	2798.03	1.41
500	34573	Superficial	0	44.58	500	3845.35	1.41
480	135397	Superficial	0	32.07	480	3130.88	1.35
480	189930	Superficial	0	13.21	480	2009.11	1.35
450	351955	Internal	92.88	123.36	438.64	4526.66	1.24
450	633796	Superficial	0	53.69	450	3797.81	1.27
450	236202	Superficial	0	70.55	450	4348.71	1.27
430	211016	Superficial	0	49.10	430	3551.26	1.21
430	617729	Internal	6.16	40.22	430	3141.80	1.21
400	220924	Internal [c]	72.12	119.23	385.57	4063.24	1.09
400	200956	Superficial	0	101.12	400	4846.51	1.13
380	517326	Superficial	0	35.83	380	2619.55	1.07

[C] In these tables, it stands for colony inclusion.

Table 5. Fatigue test results for AISI 304 steel samples with a hardness of 170 Vickers.

Stress (MPa)	Number of cycles	Place of departure	d (μm)	$\sqrt{area}$ (μm)	Stress on inclusion (MPa)	$K_{I_{max}}$ (MPa$\sqrt{m}$)	σ_a / σ_w
300	70316	Internal	119.59	65.68	282.06	2154.16	1.25
300	14905	Internal	94.64	131.05	285.82	3042.86	1.25
270	80970	Internal [c]	201.69	162.38	242.77	3161.37	1.08
270	250206	Internal	42.09	45.49	264.32	2096.53	1.17
250	656826	Internal	55.76	44.67	243.03	1539.65	1.08
250	80756	Superficial	0	54.45	250	2124.88	1.11
250	530285	Internal	348.58	71.27	206.43	1869.89	0.92
230	300449	Internal	5.34	20.42	229.39	1449.02	1.01
220	275074	Internal [c]	47.95	93.35	218.93	2083.30	0.97

[C] In these tables, it stands for colony inclusion.

In Fig. 6. the relationship between the inclusion effective area parameter (√area) and the number of cycles endured by the sample (N_f) is displayed in three steels. According to this diagram, it can be concluded that the increasing size of the inclusion causing the failure decreases in the number of cycles endured by the fatigue test specimen. However, this diagram has several examples of violations, such as the increase in the inclusion size. The sample has endured a significant number of cycles. For instance, some samples with a hardness of 330 could withstand more than 1.1×10^6 cycles despite including the effective area parameter being 57.51 micrometers. Also, Fig. 7. shows the relationship between the stress intensity factor resulting from the inclusion of the fracture agent, $K_{I_{max}}$, and the number of cycles the sample (N_f) endured in all three steels. The trend of this graph shows well that with the increase of the stress concentration resulting from the presence of inclusions in the part, the cycle endured by the sample decreases. In Fig. 7. unlike Fig. 6. there is no exceptional case, which is the use of the stress intensity factor in the diagram, which includes both stress factors imposed on the inclusion and the size of the inclusion. As a result, both critical factors in stress concentration and specimen failure are included here. Therefore, according to this diagram, it can be concluded that the best criterion for checking the strength and fatigue relationships of a sample is to use the stress concentration parameter.

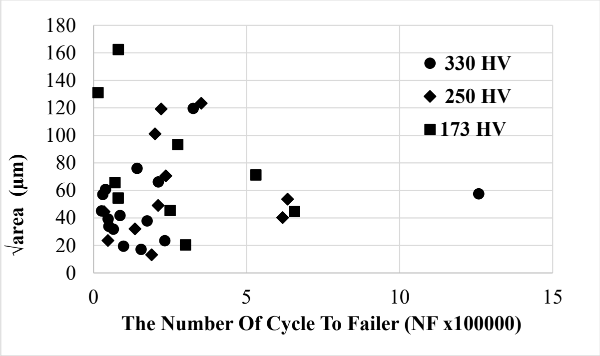

Fig. 6. The relationship between the inclusion effective area parameter (√area) and the number of fatigue cycles endured (N_f) by samples with 330, 250, and 170 Vickers hardness.

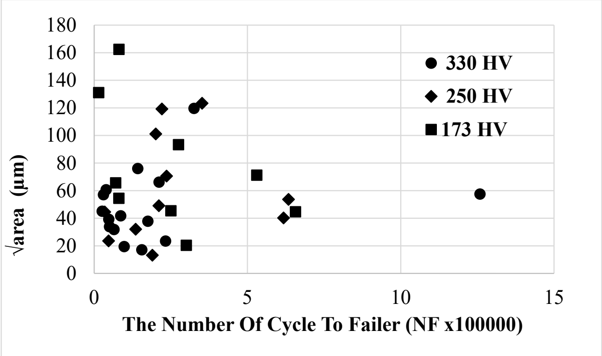

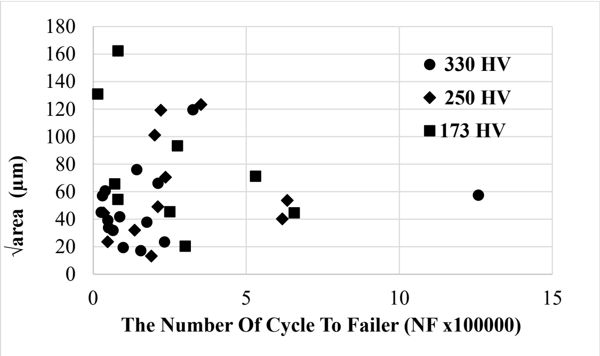

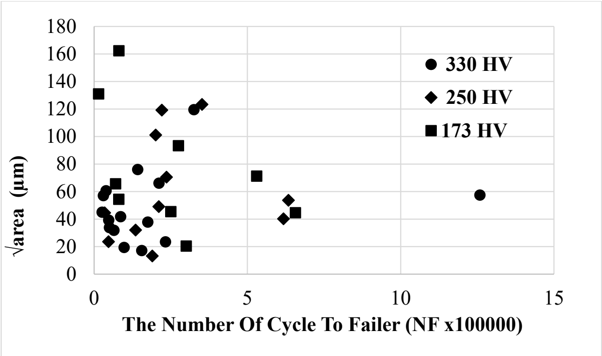

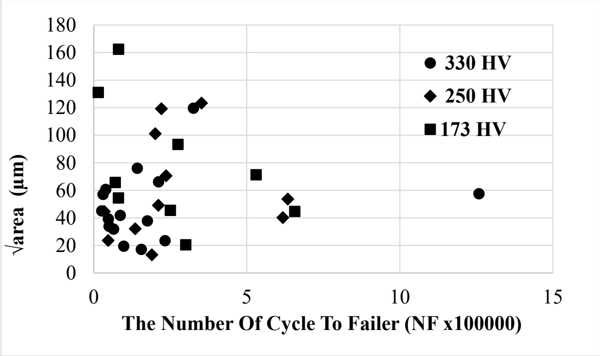

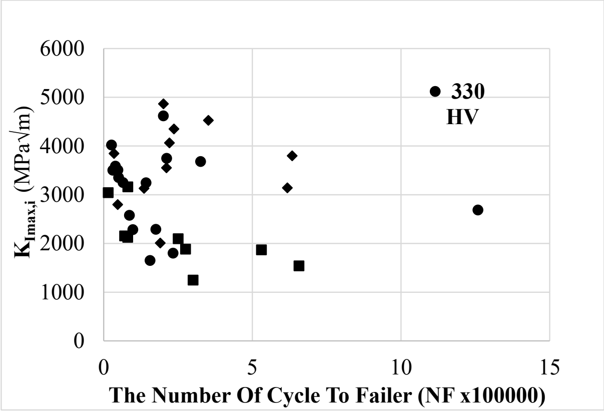

Fig. 7. Relationship between inclusion stress intensity factor ($K_{Imax,i}$) and number of fatigue cycles endured (N_f) by samples with 330, 250, and 170 Vickers hardness.

3.4. Critical inclusion size

Researchers found that there is a critical size for inclusions [16-20]. If the size of inclusions in steel is smaller than this critical size, these inclusions are no longer the source of fatigue cracks. Therefore, these inclusions are called critical inclusions. In this research, three methods, including extrapolation methods, the relationships of Murakami et al. [21, 22], and the method proposed by Saberifar [23], were used to calculate the critical inclusion size, which we will discuss further:

3.4.1. Determining the critical inclusion size by extrapolation method

In Figs. 8, 9, and 10. the inclusion effective area parameter (√area) is plotted against the inclusion distance from the sample surface for steel with a hardness of 330, 250, and 170 Vickers, respectively. According to the results obtained from these figures, the critical size of inclusion for steel with a hardness of 330, 250, and 170 Vickers equals 11.1, 13.2, and 20 microns, respectively.

The results obtained for the critical inclusion size from the extrapolation method are less reliable. This is because, in the extrapolation method, the obtained results

strongly depend on the distance of the inclusion from the surface and its size. As a result, if the location of the inclusion is changed or its size is changed, the obtained results will change. For example, adding more samples with different inclusions will change the results obtained in the following tables. Therefore, the determined critical inclusion size will also change. As a result of fatigue test results for steel with hardness of 170, 250, and 330, the extrapolation method is not a reliable method to determine the critical inclusion size.

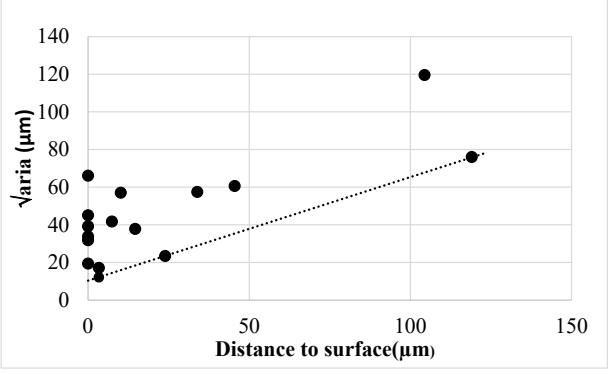

Fig. 8. Determining the critical inclusion size for steel with a hardness of 330 Vickers using the extrapolation method.

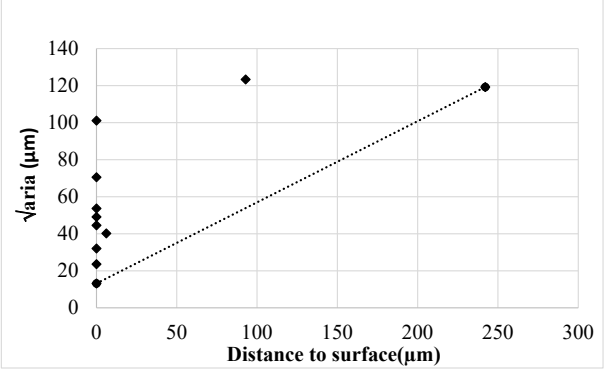

Fig. 9. Determining the critical inclusion size for steel with a hardness of 250 Vickers using the extrapolation method.

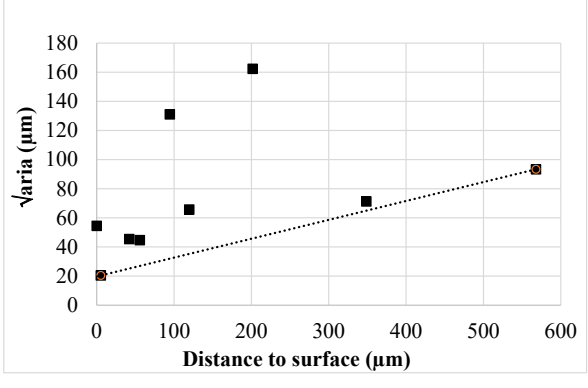

Fig. 10. Determining the critical inclusion size for steel with a hardness of 170 Vickers using the extrapolation method.

3.4.2. Determining the critical inclusion size with Murakami relations

Using Eq. (6) and examining the hardness of the sample, the critical inclusion size for steel with a hardness of 330, 250, and 170 Vickers equals 5.1, 8.5, and 19.2 micrometers, respectively. In this equation, the only effective factor in determining the size of the critical inclusion is the Vickers hardness of the sample and the location of the inclusion, and other effective factors, such as the applied stress on the part, the type of inclusion, etc., are not considered. As a result, this relationship does not have a high value. So, the results of this method cannot be an accurate and acceptable criterion for determining the critical inclusion size in industrial steels.

3.4.3. Determining the size of the critical inclusion with the relationship proposed by Saberifar

By placing the results obtained from the fatigue test, the fatigue limit for samples with hardness of 330, 250, and 170 Vickers equals 370, 350, and 220 MPa, respectively. On the other hand, according to the data in three tables 3, 4, and 5, the lowest stress intensity factor (K_{Imax}) for these three steels is 1449.02, 1650.99, and 2009.11, respectively. As a result, by inserting these values in relation 7, the value of $\sqrt{area_c}$ for samples with hardness of 330, 250, and 170 Vickers equal to 15, 24.8, and 32.7 micrometers are obtained. Assuming that the inclusion is spherical, the diameter of the inclusion is 16.94, 27.11, and 36.15 µm, respectively. If compare the numbers obtained for $\sqrt{area_c}$ with the inclusion size effective in the failure of fatigue parts, it is clear that these numbers are smaller than almost all inclusion values that caused the failure. As a result, if it is possible to obtain samples with inclusions that are smaller than the numbers obtained from the relations proposed by Saberi, it can be hoped that the inclusion will not affect the fatigue strength of the sample.

4. Conclusions

- The images obtained from the SEM microscope clearly showed that the main source of failure in the fatigue test samples is the presence of non-metallic inclusions in the sample.
- The distance of the inclusion from the surface and the size of the inclusion is one of the most important parameters in determining the fatigue limit of steel. The smaller the inclusion size, the higher the fatigue strength of the sample.
- Except for the size of inclusion, the distribution of inclusions in the part is another important parameter in fatigue strength. If the inclusions are homogeneously distributed in part, the part will have more fatigue strength.

- Besides inclusions, sample hardness is another critical parameter in the fatigue strength of samples. The results of the S-N diagram in this study show that the lower the hardness of the sample, the lower the fatigue strength of the sample. The fatigue limit for samples with a hardness of 170, 250, and 330 equals 225, 355, and 385 MPa, respectively.
- There is a critical inclusion size that. If the inclusions are smaller than this value, they no longer affect the fatigue strength of the sample. The critical inclusion size for samples with a hardness of 170, 250, and 330 equals 15, 24.8, and 32.7 micrometers, respectively.

References

[1] Gao Y.K, Li X.B, Yang Q.X, Yao M, Influence of surface integrity on fatigue strength of 40CrNi2Si2MoVA steel, Materials Letters. 2007; 61(2): 466-469.
[2] Cong T, Qian G, Zhang G, Wu S, Pan X, Du L, Liu X, Effects of inclusion size and stress ratio on the very-high-cycle fatigue behavior of pearlitic steel. International Journal of Fatigue. 2021; 142: 105958.
[3] Ferro P, Fabrizi A, Berto F, Savio G, Meneghello R, Rosso S, Defects as a root cause of fatigue weakening of additively manufactured AlSi10Mg components, Theoretical and Applied Fracture Mechanics, 2020; 108: 102611.
[4] Zhu X, Dong Z, Zhang Y, Cheng Z, Fatigue life prediction of machined specimens with the consideration of surface roughness, Materials. 2021; 14(18): 5420.
[5] Ye X.W, Su Y.H, Han J.P, A state-of-the-art review on fatigue life assessment of steel bridges, Mathematical Problems in Engineering. 2014; 2014: 1-3.
[6] Zhang L, Thomas B.G, Inclusions in continuous casting of steel, InXXIV National Steelmaking Symposium, Morelia, Mich, Mexico. 2003; 26: 28.
[7] Wang Z, Xing Z, Wang H, Shan D, Huang Y, Xu Z, Xie F, The relationship between inclusions characteristic parameters and bending fatigue performance of 20Cr2Ni4A gear steel, International Journal of Fatigue. 2022; 155: 106594.
[8] Shimatani Y, Shiozawa K, Nakada T, Yoshimoto T, Effect of surface residual stress and inclusion size on fatigue failure mode of matrix HSS in very high cycle regime, Procedia engineering. 2010; 2(1): 873-882.
[9] Murakami Y, Endo M, Effects of defects, inclusions and inhomogeneities on fatigue strength. International journal of fatigue. 1994; 16(3): 163-182.
[10] Casagrande A, Cammarota G.P, Micele L, Relationship between fatigue limit and Vickers hardness in steels, Materials Science and Engineering: A. 2011; 528(9): 3468-3473.
[11] Lipa S, Sawicki J, Dybowski K, Pietrasik R, Januszewicz B, The effect of non-metallic inclusions formed as a result of deoxidation on the fatigue strength of 15CrNi6 and 16MnCr5 steel, Archives of Metallurgy and Materials. 2018: 1345-1350.
[12] Maleki E, Bagherifard S, Guagliano M, Correlation of residual stress, hardness and surface roughness with crack initiation and fatigue strength of surface treated additive manufactured AlSi10Mg: Experimental and machine learning approaches, Journal of Materials Research and Technology. 2023; 24: 3265-3283.
[13] Lipiński T, Effect of Non-Metallic Inclusions on the Fatigue Strength Coefficient of High-Purity Constructional Steel Heated in Industrial Conditions. Applied Sciences. 2022; 12(18): 9292.
[14] Murakami Y, Metal fatigue: effects of small defects and nonmetallic inclusions, Academic Press; 2019 Jun 15.
[15] Roiko A, Interaction of non-metallic inclusions, microstructure, and fatigue loading with small crack growth in high-strength steels.
[16] Murakami Y, Toriyama T, Coudert E.M, Instructions for a new method of inclusion rating and correlations with the fatigue limit. Journal of testing and evaluation. 1994; 22(4): 318-326.
[17] Saberifar S, Mashreghi A.R, Mosalaeepur M, Ghasemi S.S, The interaction between non-metallic inclusions and surface roughness in fatigue failure and their influence on fatigue strength, Materials & Design. 2012; 35: 720-724.
[18] Vasconcellos da Costa e Silva AL. Non-metallic inclusions in steels-origin and control. Journal of materials research and technology -JMR&T. 2018; 7(3): 283-299.
[19] Beretta S, Murakami Y, Largest-extreme-value distribution analysis of multiple inclusion types in determining steel cleanliness. Metallurgical and Materials Transactions B. 2001; 32: 517-523.
[20] Wilson A.D, Inclusions and their influence on material behavior, ASM International, Chicago. 1989.
[21] Zhang J.M, Li S.X, Yang Z.G, Li G.Y, Hui W.J, Weng Y.Q, Influence of inclusion size on fatigue behavior of high strength steels in the gigacycle fatigue regime, International Journal of Fatigue. 2007; 29(4): 765-771.
[22] Yang Z.G, Zhang J.M, Li S.X, Li G.Y, Wang Q.Y, Hui W.J, Weng Y.Q, On the critical inclusion size of high strength steels under ultra-high cycle fatigue, Materials Science and Engineering: A. 2006; 427(1-2): 167-174.
[23] Saberifar S, Mashreghi A.R, A novel method for the prediction of critical inclusion size leading to fatigue failure, Metallurgical and Materials Transactions B, 2012; 43: 603-608.
[24] McGuire M.F, Stainless steels for design engineers, ASM International. 2008.